High resolution 3D seismic imaging using 3C data from large downhole seismic arrays

Björn Paulsson, Martin Karrenbach, Paul Milligan, Alex Goertz, and Alan Hardin of Paulsson Geophysical Services, with John O'Brien and Don McGuire of Anadarko Petroleum Corporation explain why recording multi-component seismic data using receivers positioned deep in the earth, and closer to the target zone, can overcome many of the limitations experienced by surface 3D seismic methods

Borehole seismic surveys, commonly known as Vertical Seismic Profiling (VSP), have been an industry standard technique for several decades. In the past, however, these data have been used primarily for check-shot type velocity surveys and for reflection mapping at the well location in a one-dimensional fashion. This 1D measurement can be extended to 2D by using one or more walk-away lines of surface source points. The 2D method works well enough for imaging simple layered stratigraphy, but in a complex reservoir a full 3D data acquisition and imaging solution needs to be pursued.

Inserting seismic sensors deep into oil and gas wells, as shown in Figure 1, allows the recording of much higher frequencies as compared to placing sensors at the Earth's surface. The reason for this is simple: seismic waves have to propagate only once through the weathered layer in a confined zone near the source. In contrast, during surface seismic surveys, waves must travel through the weathered layer twice. Each traversal of the weathered layer attenuates high frequencies much more than the low frequencies, thus reducing the image resolution. The frequency content of borehole seismic data is typically more than twice that of surface seismic data, which provides an increase in subsurface resolution.

In addition to recording higher frequency data, borehole seismic sensors provide a number of other advantages: borehole seismic data typically achieve a much higher signal-to-noise ratio than surface seismic data. The combination of a quiet borehole environment and strong sensor coupling to the borehole wall enables such high signal-to-noise ratio. Surface geophones, on the other hand, are generally poorly coupled in weathered rock and exposed to cultural and environmental noise at the surface. Good sensor coupling in the borehole enables three-component (3C) seismic data to be recorded with high vector fidelity. This ultimately allows shear and converted-wave imaging as well as the determination of anisotropy by shear wave splitting analysis (see, e.g., Maultzsch, 2003). Combining P and S wave images allows for attribute inversions of rock properties, such as fluid content, pore pressure, stress direction and fracture patterns. O'Brien et al. (2004b) use time lapse borehole seismic to map changes in such critical attributes for production monitoring purposes. Another advantage of borehole seismic surveys is a favourable geometry to illuminate complex structures such as sub-salt targets, salt flanks or steeply dipping faults.

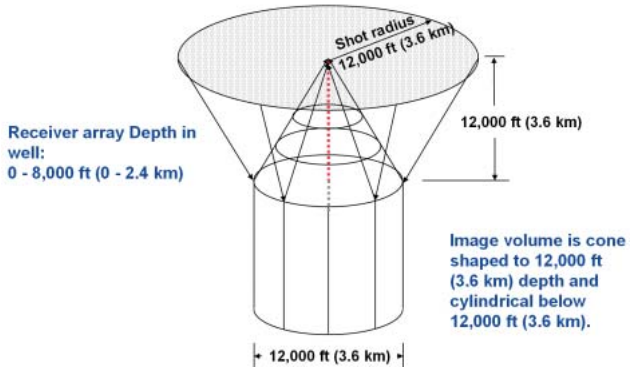

Figure 1 *Schematic view of the volume imaged by a 3D borehole seismic survey using one large vertical receiver array and a circular source pattern on the earth's surface.*

The 3D image volume that can be generated from a large downhole seismic array data is shown in Figure 1. The typical 3D borehole seismic image volume is cone shaped with the top of the cone coincident with the top receiver in the borehole array. The size of the base of the cone is determined by the depth of the image volume and the offset of the sources.

Wireline based borehole arrays

With all the advantages multi-component borehole seismic data has over surface seismic data, why has the petroleum industry not recorded more VSP data for the express purpose of 3D imaging? The answer is simple: so far, most borehole seismic arrays used on a seven-conductor wireline. Such arrays are too short and have too few channels to economically record the large data sets necessary for 3D seismic imaging. A standard seven-conductor wireline is limited to a maximum transmission bandwidth of about 500,000 bit/second, which limits the number of levels in the borehole to 16 3C levels (48 channels) if a 2 ms sampling rate is used. On the other hand, frequencies of 200 Hz or more can be recorded in a borehole from surface sources (McGuire et al.,

© 2004 EAGE

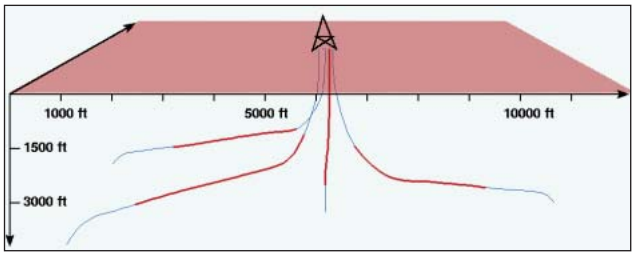

Figure 2 *Example of four 80 level receiver arrays deployed simultaneously into four highly deviated wells, starting from a common well pad; active receiver sections are shown in red, and well trajectories are shown in blue.*

Figure 3 *A work-over rig deploying the production tubing to which the downhole receiver array is attached.*

2004). In such a setting, a sampling rate of 1 ms or smaller is required, thus, limiting the number of 3C geophone levels to eight or even to four, if a sampling rate of 1/2 ms is required.

Tubing deployed borehole seismic arrays.

In order to overcome the previous limitations in borehole array technology, both the number of channels simultaneously recorded, and the data transmission rate needed to be increased. These goals have been achieved with a proprietary method deploying 3C geophone sensors attached to downhole tubing and providing a dedicated channel for each sensor component at each receiver level. With the advent of large tubing-deployed arrays, 3D borehole seismic imaging has become a viable and economic option. Images created from these surveys usually surpass surface seismic images in terms of accuracy and resolution. Current tubing-deployed technology makes it possible to deploy up to 1200 channels in one or more wells (O'Brien, 2004). Furthermore, by distributing several large downhole arrays over a larger area, the image volume can be increased. This concept is shown in Figure 2, where four wells were occupied in a survey on the

Figure 4 *A geophone pod inside the geophone pod housing. The geophone pod housings are spaced 50 ft, and connected by two tubing joints.*

North Slope of Alaska (Sullivan et al., 2002). All wells in Figure 2 are deviated, some of them up to 75^0 from vertical, making it very difficult for cable array deployment without tractors. Tubing-deployed arrays on the other hand can be installed accurately and with ease in highly deviated wells.

The tubing is the structural element in the system and consists of standard production tubing joints that have been manufactured with a length tolerance of +/- 6 mm (+/-1/4 inch). The precise length tolerance and the known mechanical and thermal expansion properties of the tubing allow the precise placement of the receivers into both vertical and horizontal boreholes. The deployment of a long downhole array using a workover rig is shown in Figure 3. Figure 4 shows a close-up view of one geophone pod assembly on the production pipe.

Clamping of receivers is achieved by inflating a bladder located behind a 3C geophone pod. The pressure required for inflation is delivered through the tubing and typically reaches 0.6 - 0.7 MPa differential pressure. As an example of the resulting data quality, Figure 5 shows a raw vertical component shot gather from a survey recorded in July 2004 using the latest generation array technology. The data shown in Figure 5 are recorded from the surface down to a depth of 5500 ft using 25 ft spacing between receiver levels. This was achieved by using a 2000 ft long 80 level downhole array with a 25 ft receiver spacing. The entire array was moved three times and recorded a 2 lb shot of dynamite in 20 ft boreholes each time.

Survey design and pre-survey modelling

One of the challenges in designing a 3D borehole seismic survey is to ensure uniform illumination in the target volume around the receiver wells. As shown by Van Gestel et al.

© 2004 EAGE

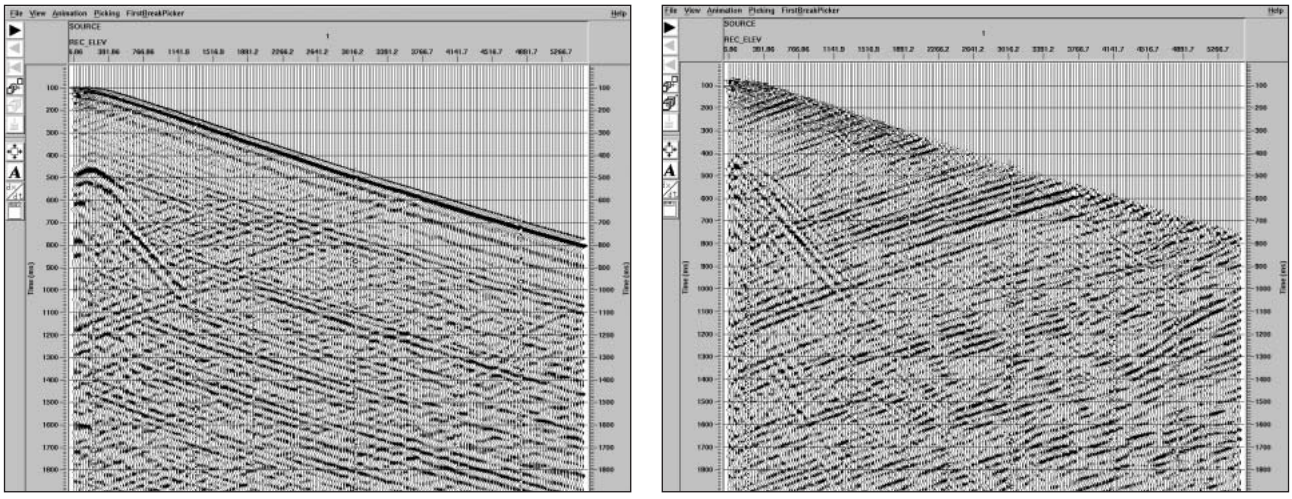

Figure 5 *(a) raw unprocessed, and (b) up-going wavefield separated shot record of the vertical component recorded by a long downhole receiver array. There are 320 receiver levels, acquired with an 80-level array in four consecutive deployments. The source consisted of a 2 lb dynamite charge close to the well. Note the high signal to noise ratio on reflected energy in the raw data.*

(2002, 2003), a sufficient receiver array aperture (i.e., array length) is critical to ensure artifact-free 3D imaging since the image size and resolution depend on the length and spacing of the borehole receiver array for a given source layout. Generally, the longer the array, the larger the volume over which good illumination can be achieved. At the same time, a dense receiver spacing is needed in order to avoid aliasing at the high frequencies obtained in the borehole environment.

In addition, the target illumination strongly depends on the distribution and spacing of the energy sources at the surface. An optimal placement of source points is necessary to achieve uniform fold coverage in the image volume around the receiver wells. Using the concept of Fresnel Volumes (Kravtsov & Orlov, 1980; Goertz et al. 2003) the minimum bin size is calculated and thus a minimum shot spacing is determined for non-aliased imaging at a given frequency. Given a uniform background velocity model and a single vertical receiver well, this optimization method results in a gradually increasing shot spacing away from the receiver well, as depicted in Figure 6. This adaptive shooting pattern requires approximately 30% fewer shot points compared to a conventional grid of equally spaced source locations while maintaining the same illumination and image resolution.

Figure 6 depicts the survey geometry and the target horizon in a gas reservoir. Pre-survey modelling of the expected hit count and angle coverage was carried out using wavefront ray tracing (Vinje et al., 1996) in an existing 3D velocity model. The hit count is obtained by counting the number of specular rays per bin cell on the target horizon (Figure 7a). Analyzing the hit count gives an estimate of the extent of the conical image volume at the reservoir level based on the

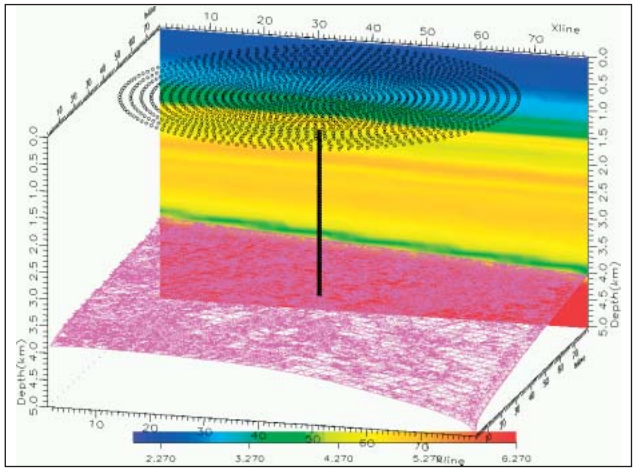

Figure 6 *Optimized survey geometry for a single-well seismic survey. The reservoir horizon is located just below the receiver array. P-wave velocities from a 3D model are colour-coded on a slice through the volume. The shot spacing increases with offset from the well head as a consequence of the Fresnel zone coverage on the target horizon.*

shape of the horizon and the 3D velocity model. As a rule of thumb, the image area at the target is about half the maximum shot offset (see Figure 1).

Of particular interest in borehole seismic reservoir characterization is the capability to invert the dynamic properties of the reflected wavefield by means of Amplitude versus Offset or Angle (AVO/AVA) analyses. Aside from a controlled recording environment and data processing for the proper handling of seismic amplitudes, this requires a sufficient and uniform aperture within the image volume in order

© 2004 EAGE

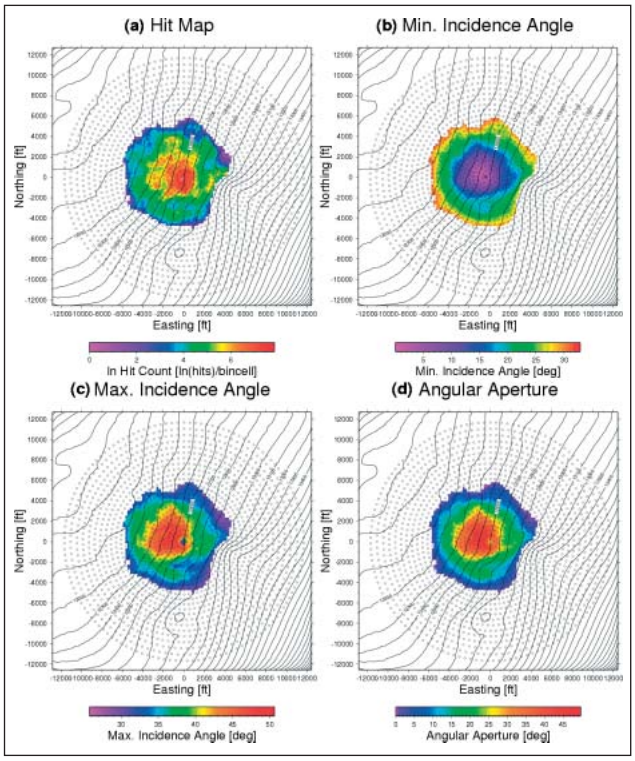

Figure 7 *Result from pre-survey modelling for the acquisition geometry depicted in Figure 6. Open circles indicate source points at the surface, and black lines represent depth contours of the target horizon. Part (a) shows the hit distribution, (b) shows minimum incidence angle, (c) shows maximum incidence angle, and (d) shows angular aperture on the target horizon.*

to extract AVO gradients over a range of incidence angles. In a borehole, reflection amplitudes are generally measured more reliably than at the surface since the reflected wavefield is not distorted by the weathering layer and often the receivers are clamped to a cemented borehole casing. However, the angular illumination for a 3D borehole seismic survey is typically less uniform than for a surface seismic grid. Therefore, the range of incidence angles observed at each image point has to be assessed beforehand. For such detailed studies, Figures 7b) and c) depict the minimum and maximum incidence angles at which an image point on the target horizon is illuminated. By subtracting the minimum and maximum incidence angle we obtain an angular aperture (Figure 7d), which gives an estimate of the range of angles over which AVA information can be gathered.

Pre-survey modelling is a critical step for ensuring that the 3D reservoir imaging objectives will be met. The parameters that need to be determined in the survey design phase are the receiver array spacing, the receiver array aperture and the source layout needed to image a target reliably with a desired resolution.

3D imaging of large downhole array 3C data

The use of large tubing-deployed downhole receiver arrays enables sufficient aperture and sampling density for high-resolution imaging in 3D. Seismic data using long downhole arrays may have been simultaneously recorded from multiple wells equipped with several hundreds of channels, and these wells may be highly deviated from vertical. Keeping in mind the massive amount of data created from such surveys, it becomes obvious that there must be some departures from traditional VSP data processing.

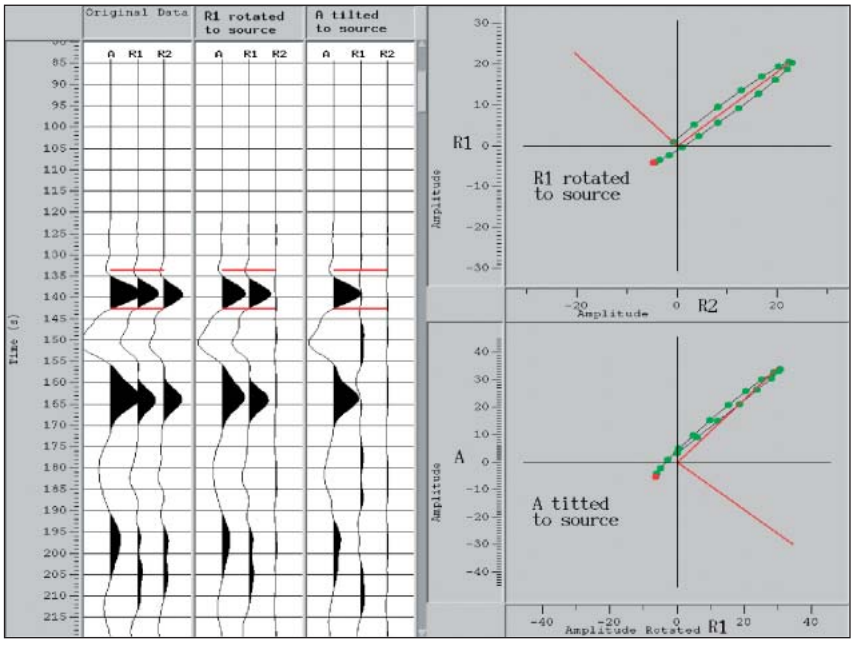

Figure 8 *Hodogram analysis is used to determine receiver component orientation. Left trace panel is raw 3C data, with Axial, first radial (R1), and second radial (R2) components respectively. Centre trace panel is after rotation of the R1 component towards the source in the plane perpendicular to the borehole. Right trace panel is after rotating the R1 component, and after tilting the Axial component towards the source. Since the axial component's orientation is known from the well deviation survey, we only need the rotation angle required to maximize source energy in the R1 component, corresponding to the upper hodogram. The Hodograms on the right show excellent vector fidelity.*

© 2004 EAGE

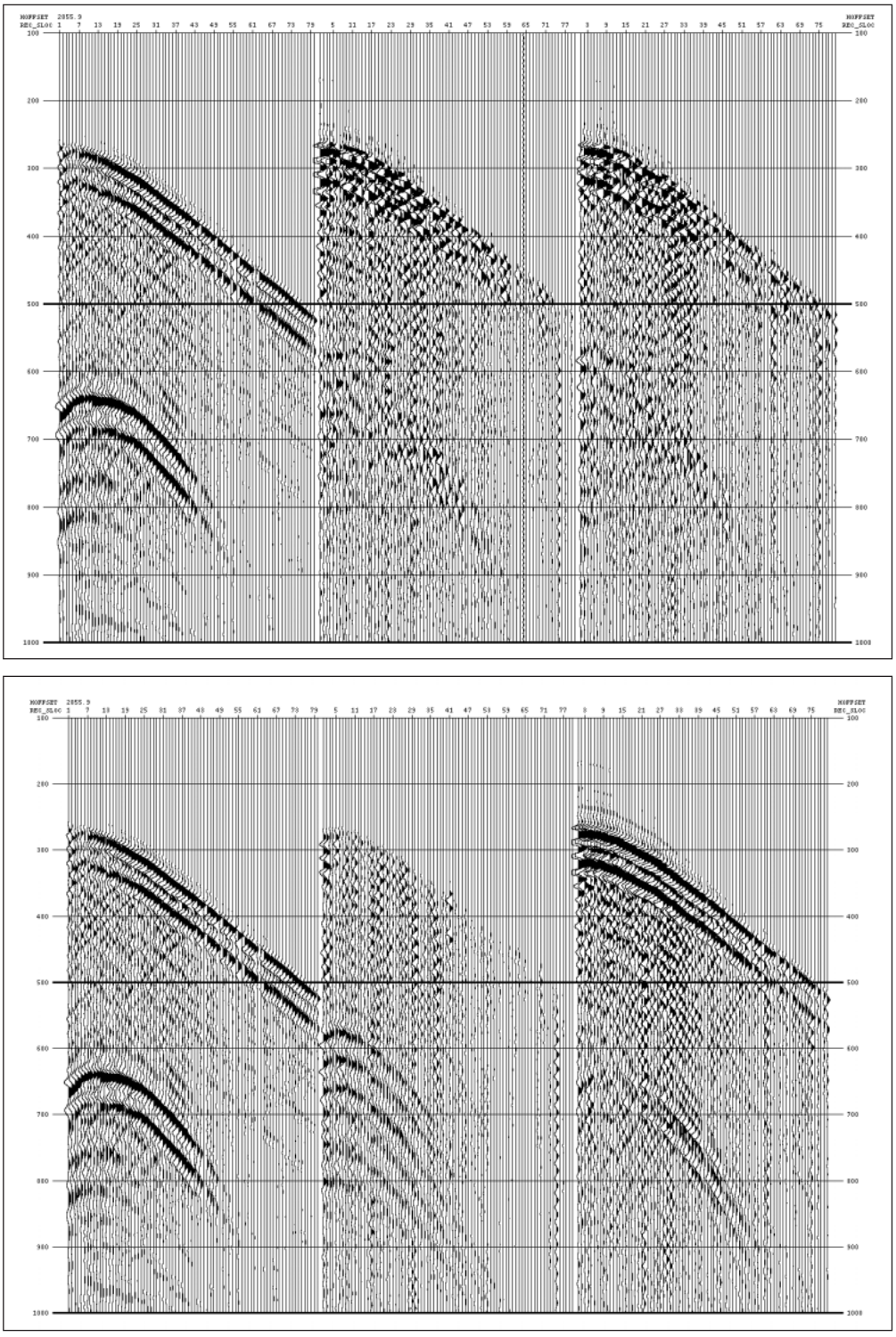

Figure 9 *Raw 3C shot record (a) before rotation; components are Axial, Radial1, Radial2; (b) after rotation to true XYZ; the axial component is now vertical (Z), the radial1 component is now pointing due east (X), and the radial2 component is pointing due north (Y). We may re-label these components as V, H1, H2 respectively. This particular source was located 2055 ft due east of the receiver well, so there is maximum direct wave arrival energy on the H2 component, and minimal on the H1 component (which points due north).*

© 2004 EAGE

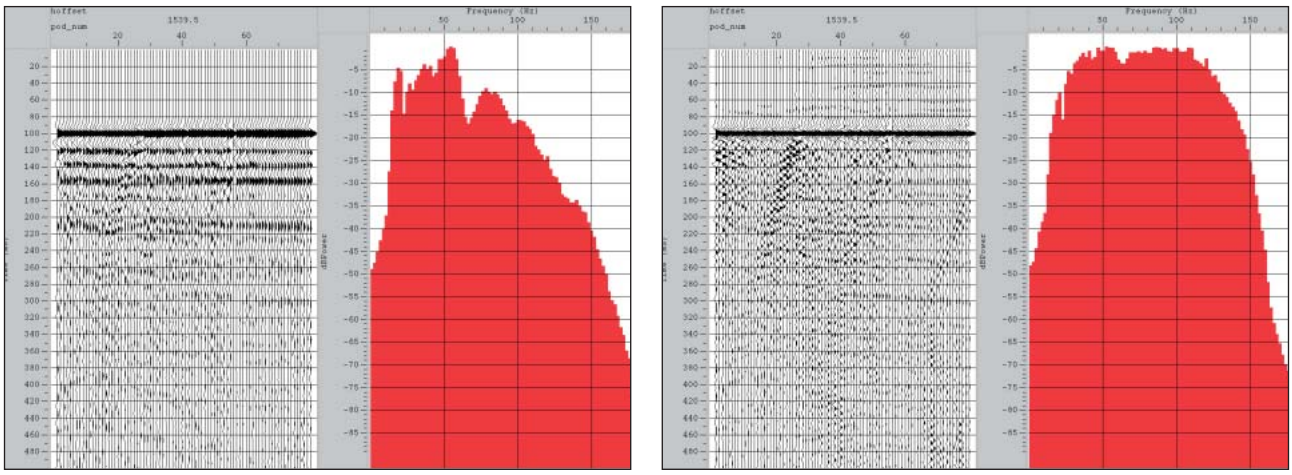

Figure 10 *Spectra of a shot record's vertical component rotated towards source and aligned on FB picks; (a) before source signature deconvolution; (b) after source signature deconvolution. In this case we used a zero phase wavelet inversion method based on the first 200 ms.*

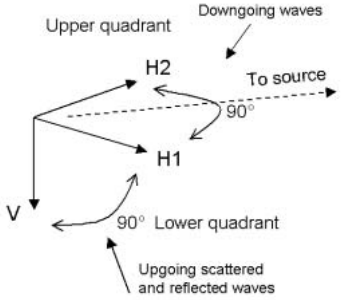

Figure 11 *Geophone component orientation used for 3D-3C wavefield separation. The 3-components are oriented so as to split the source azimuth equally between the H1 and H2 components, while the vertical (V) component remains vertical. The desired upgoing wave mode is expected to arrive from anywhere in the lower 3D quadrant in the source direction.*

Multi-component orientation

The first departure from traditional VSP processing is the computation of receiver geophone vector orientations. Since arrays do not use gimbal-mounted geophones, the two radial components are randomly oriented after deployment and clamping in the well. However, once deployed and clamped, the long downhole arrays remain in place for the duration of the 3D survey, allowing the orientation of the radial components to be obtained accurately by averaging over a subset of shotpoints.

The orientation of the two radial receiver components is determined with a hodogram analysis on the first-break arrivals for a subset of shot points. For a vertical well, a circle of shot points at similar offset to receiver depth is chosen. Using a full circle helps mitigate the possibility of ray bending caused by lateral velocity changes. However, for a highly deviated well, it is possible to place a walk-over line of shot points directly over the receivers. The advantage of using a walk-over line for hodogram analysis is the relatively straight direct ray paths taken by the first arrivals, leading to less ambiguity in radial component orientation. Figure 8 shows a typical hodogram analysis for receiver component orientation from a single shot point.

Once the hodogram analysis is complete, and all receiver orientations are known, the next major processing step is to rotate the entire 3C raw data set into true XYZ orientation. This results in a new 3C data set with components orientated due east, due north, and vertical, respectively. The separate components of a typical shot gather are shown in Figure 9a before rotation (Axial, radial1 and radial2), and in Figure 9b after rotation to true XYZ (H1, H2, V).

Processing continues with first-break (FB) time picking followed by source signature analysis and deconvolution filter computations. To facilitate both FB picking and source signature analysis, the 3C data are rotated to enhance either the direct P-wave component, or the direct S-wave component. The resulting deconvolution filters are both surface-consistent and deterministic, and result in a common wavelet suitable for pre-stack depth migration (PreSDM). Figure 10 shows an example comparing a typical shot-gather before (a) and after (b) deconvolution and bandpass filtering. The FB pick times are used later for velocity model construction and for computing 3D source statics.

Multi-component wavefield separation

The second main departure from traditional 2D VSP data processing is the method for wavefield separation prior to 3D imaging. Wavefield separation attempts to isolate reflected up-going and scattered energy, which is then used as input to scalar Kirchhoff pre-stack depth migration (PreSDM).

Traditionally, wavefield separation for 2D VSP reflection

© 2004 EAGE

imaging has been done by focusing on primary reflections within the source-receiver vertical plane, either directly by maximizing reflected signal strength, or indirectly by maximizing signals arriving at the expected angle of primary reflections from horizontal layers. Both 3C rotation and array beam steering methods can be used to achieve this.

However, reflection and diffraction energy arrives from many different angles within the volume to be imaged, and all of these arrivals should be used to construct the image. Thus it is desirable to keep the receiver antenna aperture open as wide as possible in all three dimensions to enable recovery of all possible scattered/reflected events. Consequently, the 3D-3C wavefield separation technique accepts the desired up-going wave mode from as wide an incidence angle range as possible (ideally with an isotropic response), while also attenuating the undesired down-going wave mode.

The 3D-3C wavefield separation process begins by rotating the horizontal components towards the source (see Figure 11). The three components are then mathematically combined to accept the desired up-going wave mode with unit response regardless of angle of arrival within the lower 3D quadrant, while also attenuating the undesired down-going wave mode arriving in the upper quadrant. The attenuation is at a maximum if the undesired down-going wave arrives with a 45^0 incidence angle, otherwise it is attenuated with a dipole response curve (see Figure 12). Remaining down-going direct arrival energy is maximized on the first break after deconvolution and can be muted. The polarity of the components are then switched to select the up-going wave mode, i.e., up-going P, or up-going SV, while the complementary down-going wave mode is attenuated. In areas with strong wave mode conversions, there is one caveat: separation of upgoing P-P events can be contaminated by down-going P-S events, and vice versa. If these unwanted wave modes are producing image artifacts after stacking, then tau-p filtering is necessary to suppress them before migration.

In addition, this 3D-3C wavefield separation technique allows the tilting of all 3C axes while maintaining orthogonality, allowing it to deal with the case of a deviated (non vertical) well where a receiver may be directly below a surface source point. At this vertical angle, traditional 3C VSP wavefield separation must resort to velocity filtering, or beam-steering the receiver array, which effectively narrows the receiver antenna aperture and adversely attenuates reflection/diffraction arrivals from elsewhere. This can be detrimental for imaging complex structures in 3D, such as small stratigraphic faults, pinch-outs, or channel edges.

Surface-borehole 3D statics

3D statics for surface-to-borehole seismic are an inherent problem without an accurate shallow layer velocity model. Because all the receivers are usually below the weathered layer and only occupy a small lateral area it is impossible to use established methods, such as refraction arrival move-out or turning ray tomography to map weathered layer velocity or thickness changes over the area covered with source points. Instead, ray-tracing is used to compute the source-receiver direct arrival times in an estimated velocity model. The computed arrival times are compared to the actual FB pick times. Filtered differences between picked and computed arrival times for any one source can be averaged and applied as a static correction, as illustrated in Figure 13.

This model-driven static solution may include corrections for imperfections in the velocity model located between the source and receiver well, instead of being strictly local to the source point. Therefore, a static solution is obtained that is intrinsically tied to a given velocity model, and any velocity model update automatically requires a statics solution update.

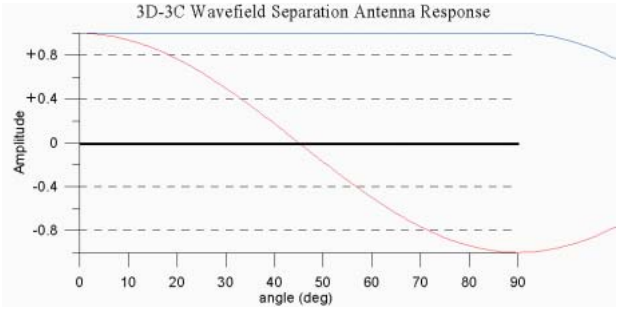

Figure 12 *The resulting receiver antenna angular response after wavefield separation. The 0-90° scale represents either the horizontal or vertical plane in the lower or upper 3D quadrant pointed towards the source. The red curve is the attenuation response of the unwanted (down-going) wave. The blue curve is the desired (up-going) wave mode response. It can be seen that at an incidence angle of exactly 45^0, there is maximum attenuation of the down-going wave.*

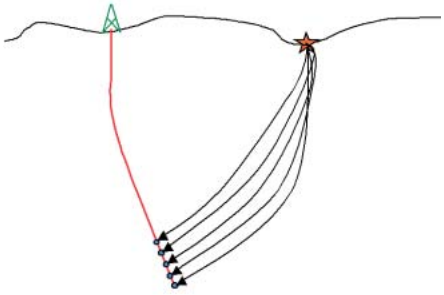

Figure 13 *Surface-to-borehole shot statics takes the average of several travel time differences between ray traced arrival times and picked first break arrival times, common to a shot, into a group of (n) lower receiver levels. Static value is a function of the average difference: 1/n* Σ *(FBcomputed – FBpicked).*

© 2004 EAGE

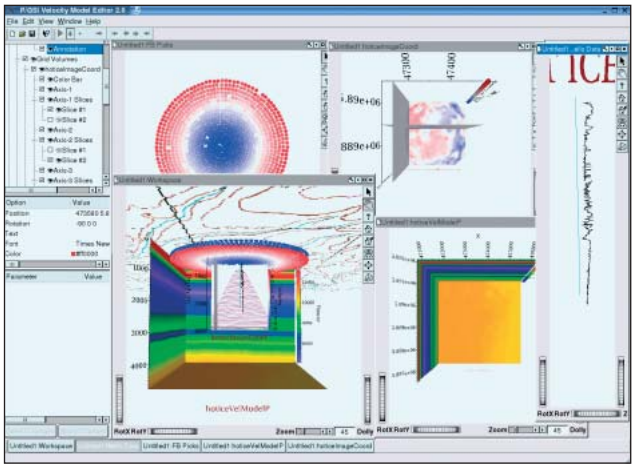

Figure 14 *Composite 3D display and detailed views of integrated data sets for velocity model building. Auxiliary information is combined with data and processing results to enable interactive model changes and quality control.*

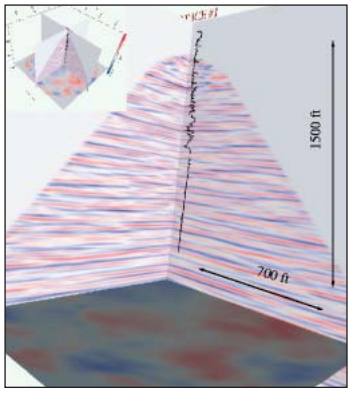

Figure 15 *3D view into a high-resolution image of a methane hydrate target from the North Slope of Alaska, including an integrated well log. The well was cased in the upper part and uncased in the lower part. The 3D depth image accurately ties with the well log in minute detail, and allows detailed interpretation away from the well.*

Velocity estimation and pre-stack depth migration

Following these pre-processing steps, the wavefield-separated and amplitude-balanced data are pre-stack depth-migrated using a Kirchhoff imaging method. Due to the illumination pattern for a 3D borehole seismic survey, it is favourable to parameterize the migration algorithm in terms of incidence angle at the image point. This allows re-sorting the migrated data into the incidence angle domain such that common-angle gathers can be obtained for both velocity model update as well as AVA studies. For a kinematic structural image, partial pre-stack depth-migrated images are combined to form complete P-P or P-S reflection image volumes.

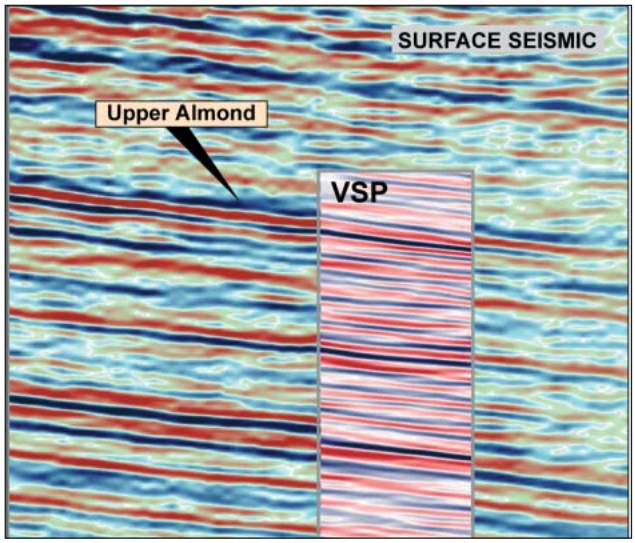

Figure 16 *Comparison depth slice of a 3D surface seismic image, with a 3D VSP image slice at the same location. Note the increased resolution and detail of the 3D VSP image.*

Depth imaging is sensitive to the velocity model, and great care must be taken in building the 3D velocity volume. An interactive velocity model building tool is used to achieve this in an iterative manner. Both VSP data and geological constraint data are used. Interpreted horizons or other a priori constraints can also be imposed. Both direct-wave and reflected-wave tomography and event move-out analysis in the depth domain are used. Common angle gathers at an image point in the depth domain are used for this move-out analysis.

The velocity model estimation is iterative in nature and uses interactive velocity model manipulation tools (see Figure 14) to produce model updates. It is important to use all auxiliary information available from the survey site, including well logs, formation tops, horizon information, ray path computations, velocity models and migrated image volumes, and to analyze them within a common framework. Only then can the interpretive processing procedures be used efficiently to obtain a velocity model accurate enough for PreSDM. In the following, we illustrate the 3D VSP methodology with two case studies that demonstrate the range of applications this technology is suited for.

High-resolution 3D imaging for methane hydrates exploration

A 3D VSP survey was recorded in February 2004 in conjunction with a continuously cored hydrate exploratory well (Hot Ice #1) on the North Slope of Alaska (McGuire et al., 2004). The purpose of the VSP was to identify and delineate lateral variations in the subsurface within the hydrate stability zone (HSZ) by using high frequency seismic sources arrayed in a 3D surface pattern and a large receiv-

© 2004 EAGE

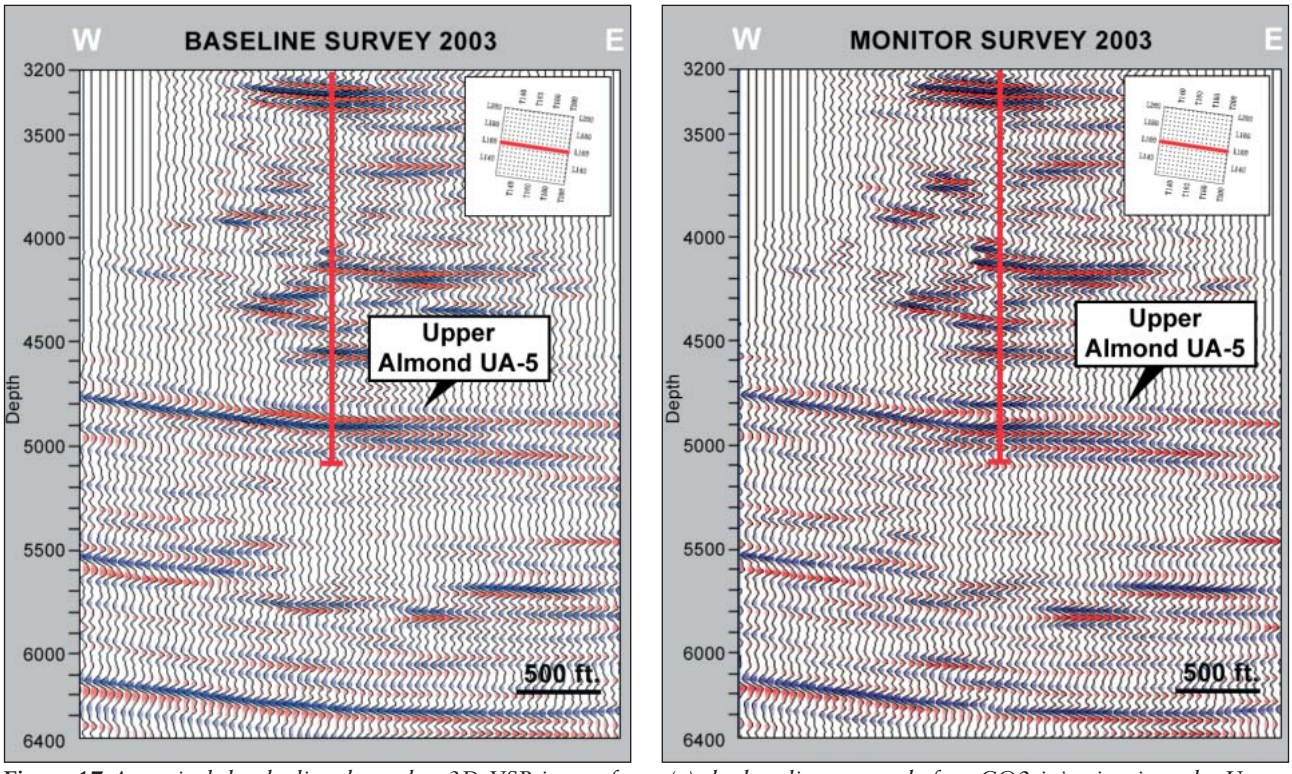

Figure 17 *A vertical depth slice through a 3D VSP image from (a) the baseline survey before CO2 injection into the Upper Almond formation, and (b) after CO_2 injection. Note the distinct change in reflectivity around the well.*

er array in the wellbore. Pre-survey modelling indicated that only a 3D downhole seismic survey would yield a high enough dominant frequency to successfully image the thin hydrate bearing layers.

The seismic source signal was composed of two 10 second linear sweeps from 8-220 Hz transmitted from each of 1185 surface locations. The seismic data were recorded by an 80-level 3C borehole array with a geophone spacing of 25 ft.

In Figure 14, an integrated, interactive velocity model-building tool has been used to analyze the Hot Ice #1 data. The main window shows the high resolution 3D image volume immersed in the 3D velocity model that was used for the PDSM. The circular source pattern shows colour-coded first arrival times and is displayed together with the sonic log. Figure 15 selects an overall view of the 3D image volume. The sonic log is draped in the centre of the cone shaped 3D image. The depth slice at about 2200 ft depth below the earth surface shows in detail the patchy nature of the amplitude distributions at this target level.

The close-up view into the volume shown in Figure 15 shows the excellent correlation between the well log sonic curve and the depth image. The well log shows two sections of distinct character. The upper section corresponds to the cased portion of the borehole, and the lower section representing the un-cased part of the borehole. The high-resolution 3D image proves consistent over the entire borehole range and correlates very well with the velocity contrasts seen in the sonic curve.

High-resolution time-lapse 3D imaging

In 2001 Anadarko Petroleum Corp initiated a miscible CO_2 enhanced oil recovery project in the Monell Unit of the Patrick Draw field in Wyoming, as reported in O'Brien et al. (2004). The objectives of this project were to test the injection process and the response of the reservoir to CO_2 injection. As part of the project, movement of the CO_2 front was monitored by time-lapse 3D VSP using a large downhole array.

A baseline 3-D VSP survey was acquired in the Monell 180 ST-1 well in January 2002 using a large downhole array, and the survey was repeated in June 2003 after 18 months of CO_2 injection. For both the baseline and monitoring surveys, a borehole array consisting of 80 receiver levels at 50 ft spacing was placed from the near-surface to a depth of approximately 4300 ft depth. A vibroseis source generated a source signal from 8 -180 Hz. Source locations extended with full azimuthal coverage to a maximum offset of about 5000 ft away from the well.

Figure 16 shows a data comparison between a surface seismic image and the 3D VSP image. While the surface seismic data have good bandwidth up to 60 Hz at these shallow

© 2004 EAGE

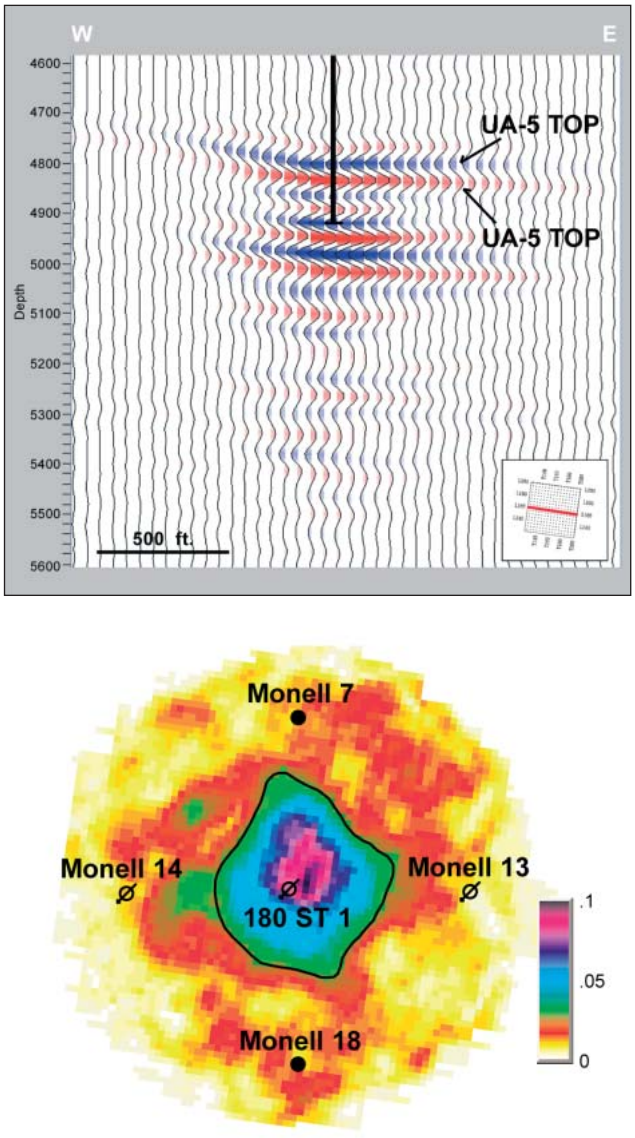

Figure 18 *a) A vertical slice at the well through the 4D cross-equalized difference between the baseline survey and post CO2 injection survey images. Note that in addition to the changes in reflectivity in the Upper Almond layer, there are also apparent changes in lower layers, and these are caused by "push-down" of these reflection events because of the post-CO2 injection velocity changes. b) A horizontal amplitude map along the Upper Almond Top UA-5 delineates in great detail and with high-signal to noise ratio the extent and direction of the CO2 flooding that occurred within 18 months.*

depths, the VSP data have a significantly higher frequency content and vertical resolution that provide more detailed imaging.

Figure 17a and b show the resulting vertical east-west slices through the 3D image volume for the baseline and monitoring surveys respectively. The images provide an excellent view of Upper Almond UA-5 reservoir and allow a detailed comparison of amplitude changes due to CO_2 injection. In Figure 18a the monitor data were cross-equalized and subtracted from the baseline data clearly delineating changes within the 42 ft reservoir interval which are attributed to the CO_2 flood. Figure 18b shows a map view of the time-lapse amplitude difference at the reservoir level. The CO_2 injection occurred in the Monell 180 well in the center. The acoustic properties of the reservoir are changed slightly as the CO_2 flood advances through the formation, giving rise to seismic amplitude changes in the 3D image. The time-lapse 3D VSP clearly documents the advance of the CO_2 flood into the reservoir providing information on the rate of advance and the azimuthal uniformity of the flood and also implying that no areas have been left unswept.

Conclusions

The use of large 3C borehole seismic arrays has evolved into a powerful technology for 3D imaging and reservoir characterization. 3D-3C borehole seismic surveys provide data with high vector fidelity and the high frequency content of the data provides imaging detail with superior vertical and lateral resolution. The excellent survey repeatability and the high signal/noise quality enable the implementation of sophisticated dynamic reservoir monitoring techniques. The ability to tie depth seismic data directly with well logs ensures accuracy and reduces uncertainties in 3D images. In contrast to surface seismic data, wave field quantities can be determined directly in depth. Several examples presented in this paper show how this technology is increasingly employed in a target-oriented fashion for the characterization of complex reservoirs that cannot be effectively imaged using surface seismic. Many stratigraphically complex areas require high resolution imaging that can be achieved only by acquiring high-frequency, high-fidelity seismic data within a borehole.

Acknowledgements

We wish to thank Paulsson Geophysical and Anadarko Petroleum Corp for permission to publish imaging results. The surface seismic data are shown courtesy of PGS Onshore. The large downhole receiver technology was supported through co-operative grant DE-FC26-01NT41234 and acquisition of the Hot Ice Methane Hydrate data through co-operative grant DE-FC26-01NT4133 by the US Department of Energy National Energy Technology Laboratory.

References

Bredbeck, T. and Buehring, R. [2003] 3D Vertical Seismic Profiles - Implications for Reservoir Characterization, Lithology and Fluid Detection. *EAGE Workshop*, Stavanger, Norway.

© 2004 EAGE

Chopra, S., Alexeev, V., Manerikar, A. and Kryzan, A., [2004] Acquisitions/Processing-Processing/integration of simultaneously acquired 3D surface seismic and 3D VSP data. *The Leading Edge*, **23**, 5, 422.

Goertz, A., Mueller, C., Buske, S. and Lueth, S. [2003] Elastic Fresnel-Volume True-amplitude Multicomponent Migration. *65th EAGE Annual Conference, Stavanger, Norway*.

Kravtsov, J. A. and Orlov, J. [1980] *Geometrical Optics in inhomogeneous media*. Springer Verlag.

Maultzsch, S., Liu, E., Li, X.-Y., Daley, T., Queen, J., Cox, D. [2004] Shear-wave splitting analysis of a 3D VSP from the San Juan Basin. *65th EAGE conference, Stavanger, Norway*.

McGuire, D., Runyon, S., Williams, T., Paulsson, B., Goertz, A. and Karrenbach, M., [2004] Gas Hydrate Exploration with 3D VSP Technology, North Slope, Alaska. *SEG 74th Annual International Meeting*.

O'Brien, J., Kilbridge, F. and Lim, F. [2004] Time-Lapse 3-D VSP Monitoring of a CO_2 EOR Flood. *SEG 74th Annual International Meeting*.

O'Brien, J., Kilbridge, F. and Lim, F. [2004] Time-Lapse VSP Reservoir Monitoring. Submitted to *The Leading Edge*.

Sullivan, C., Ross, A., Lemaux, J., Urban, D., Hornby, B., West, C., Garing, J., Paulsson, B., Karrenbach, M. and Milligan, P. [2002] A massive 3D VSP in Milne Point, Alaska. *SEG 72nd Annual International Meeting*.

Van Gestel, J. and Ray, A. [2002] VSP survey design using finite difference modeling, *SEG 72nd Annual International Meeting*, Expanded Abstracts, 2361-2364.

Van Gestel, J., Hornby, B., Ebrom, D., Sharp, J. and Regone, C., 2003, Effects of changing the receiver array settings on VSP images. *SEG 73rd Annual International Meeting*, Expanded Abstracts, 2278-2281.

Vinje, V., Iversen, E., Åstebøl, K. and Gjøystdal, H. Estimation of multivalued arrivals in 3D models using wavefront construction – Part I. *Geophysical Prospecting*, **44**, 819-842.

© 2004 EAGE